

# Correlation of the crystallization process of amorphous magnetics $\text{Fe}_{90}\text{Ni}_{10}$ and $\text{Fe}_{90}\text{Ni}_{1.5}\text{Si}_{5.5}\text{B}_3\text{P}_{0.015}$ with changes of electrical resistance and magnetic permeability

M. V. ŠUŠIĆ

*Institute of Physical Chemistry, Faculty of Science, University of Belgrade, PO Box 550, 11001 Belgrade, Yugoslavia*

A. M. MARIČIĆ

*Technical Faculty, B. Kidriča 65, 32000 Čačak, Yugoslavia*

The correlation of characteristics of the crystallization process of iron-based magnetics  $\text{Fe}_{90}\text{Ni}_{10}$  (I) and  $\text{Fe}_{90}\text{Ni}_{1.5}\text{Si}_{5.5}\text{B}_3\text{P}_{0.015}$  (II) and their relative electrical resistance and relative magnetic permeability were investigated. It is shown that the amorphous magnetics crystallize at definite temperatures in one or two steps. For these processes the kinetic and thermal parameters were determined. For Alloy I the activation energy is  $349 \text{ kJ mol}^{-1}$  and the frequency factor  $7.7 \times 10^{25} \text{ min}^{-1}$ . Alloy II shows two distinct processes with activation energies of 1193 and  $950 \text{ kJ mol}^{-1}$ , with corresponding frequency factors of  $3.6 \times 10^{76}$  and  $3.8 \times 10^{61} \text{ min}^{-1}$ . The crystallization processes are accompanied by changes in electronic and magnetic structures, leading to decreases of both electrical resistance and magnetic permeability, especially in the range of crystallization temperatures of the amorphous magnetics.

## 1. Introduction

Glassy metals have recently been considered as a particularly attractive category of metallic materials due to their outstanding physical, physico-chemical and technical properties. Many laboratory and large-scale methods for preparation of glassy (amorphous) metals and alloys in different forms (wire, ribbon, powder, etc.) have been developed. All these methods are based on rapid cooling of the metal or alloy melts, on condensation from the gaseous phase on supercold substrates, or on spraying of the melt on such media. In every case the product obtained is disordered or ordered at a short range with random packing of atoms, microsystems or clusters, as the process is viewed by different, rather discordant, theoretical models [1-6]. The seemingly dominant model [7] points out three types of processes: polymorphous, primary, and eutectic crystallization.

We wish to emphasize some significant properties of glassy metals when applied in different fields of the fundamental sciences and in engineering. Among the physical and physico-chemical properties, determining the stability of the glassy state, the temperature dependence of the electrical and magnetic properties of the glassy magnetics appears to be quite important.

Increased interest in magnetic properties can be seen in a monograph [8], but there are few data which connect the changes of magnetic and electrical proper-

ties with the crystallization process [9]. This problem is dealt with by a number of theories which differ in many assumptions, especially those concerning amorphous structures of the magnetics [1, 10, 11], crystallization and partial crystallization. The problem is quite complex because the addition of certain components (elements) can decrease or increase the value of magnetic moments, which was especially noticeable with magnetics containing rare-earths and iron in the presence of hydrogen [12]. The formation of hydrides, next to changes in magnetic characteristics, may influence mechanical properties of the magnetics, transforming them even to powders ([8] pp. 506-12). A literature review of these topics may be found in Reference 13.

## 2. Experimental procedure

The subjects of this investigation were two glassy alloys:  $\text{Fe}_{90}\text{Ni}_{10}$  (I) and  $\text{Fe}_{90}\text{Ni}_{1.5}\text{Si}_{5.5}\text{B}_3\text{P}_{0.015}$  (II), the subscripts denoting atomic per cent. They were in the form of ribbons with a thickness of 0.01 mm, obtained by rapid cooling of alloy melts by the melt spinning method. The crystallization process was monitored by differential scanning calorimetry (DSC) using a DuPont thermal analyser (1090) in a hydrogen flow. Determination of the thermal and kinetic parameters of the process was done by Šušić's method [14]

which is based on the dependence of the temperature of the exo-peak of crystallization on the heating rate

$$\beta/T^2 = (ZR/E)\exp(-E/RT) \quad (1)$$

where  $\beta$  is the heating rate ( $\text{K min}^{-1}$ ),  $T$  the absolute temperature of the exo-maximum at the DSC diagram,  $E$  the activation energy, and  $Z$  the frequency factor of the process. Equation 1 can be transformed to

$$\ln(\beta/T^2) = \ln(ZR/E) - E/RT \quad (2)$$

The dependence of  $\ln(\beta/T^2)$  on  $1/T$  is linear and the activation energy of the process is readily found from the slope, which is

$$\Delta \ln(\beta/T^2)/\Delta(1/T) = -E/R \quad (3)$$

From Equation 1 the frequency factor is

$$Z = [\beta E \exp(E/RT)]/RT^2 \quad (4)$$

The rate constant is obtained from the well-known expression

$$k = Z \exp(-E/RT) \quad (5)$$

The temperature change of the relative resistance,  $R/R_{25^\circ\text{C}}$ , was continually recorded in a hydrogen atmosphere by the four-point method. For determination of the relative magnetic permeability,  $\mu/\mu_{20^\circ\text{C}}$ , each particular sample was repeatedly heated to higher and higher temperatures and was measured after cooling to room-temperature. It was calculated from the magnetization force, the magnetic field strength and shifts of the sample position depending on the magnetic field of the solenoid, which was measured using an electronic balance.

From these data the magnetic permeability of the sample,  $\mu$ , relative to the permeability of air,  $\mu_0$ , was calculated from the equation

$$\mu = \frac{(F_1 + F_2)\Delta X}{\mu_0(H_2^2 - H_1^2)V} \quad (6)$$

where  $F_1$  and  $F_2$  are magnetic forces of the solenoid acting upon the sample along the axis of the solenoid and moving the sample from position  $X_1$  to  $X_2$ , i.e. for  $\Delta X = 1$  mm. The volume of the sample is  $V$  and the magnetic field strength,  $H$ . The values of  $\mu$  were obtained for each heating temperature, including the temperature of crystallization of the sample. In the measurements, the magnetic field strength was  $H_1 = 7160 \text{ A m}^{-1}$ ,  $H_2 = 8058 \text{ A m}^{-1}$  and the volume of the sample  $3 \times 3 \times 0.02 \text{ mm}^3$ , i.e.  $1.8 \times 10^{-10} \text{ m}^3$ .

### 3. Results and discussion

#### 3.1. Thermal and kinetic analysis

##### 3.1.1. Alloy I

The DSC thermograms show that the crystallization process takes place in one step exothermally at about  $430^\circ\text{C}$ , as seen in Fig. 1. By determining the areas of the exothermal peaks obtained at different heating rates, it is found that the enthalpy of crystallization is  $-\Delta H = 55\text{--}57 \text{ J g}^{-1}$ . The X-ray diffractograms (XRD) presented in Fig. 2 show the spectrum before (a) and after (b) of the sample crystallization. From the

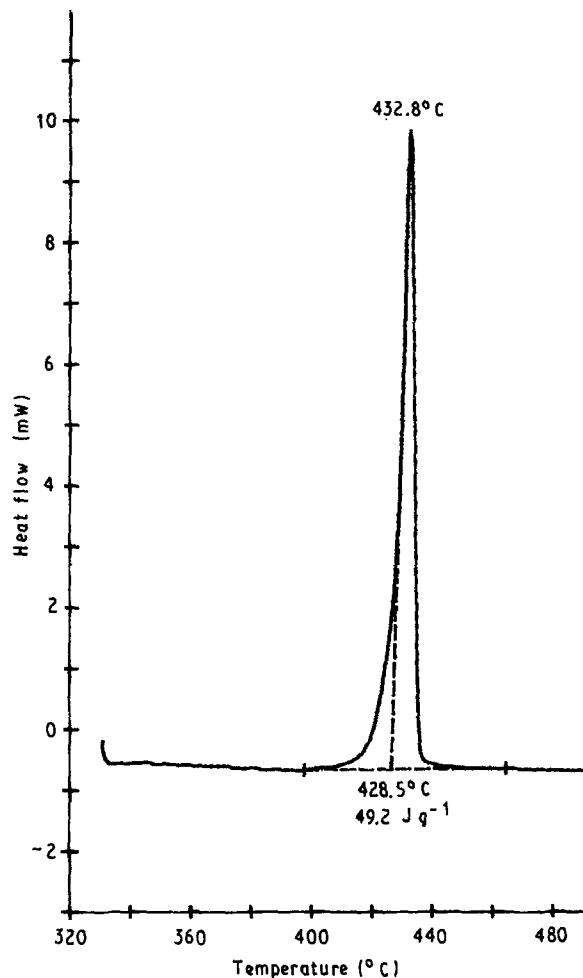


Figure 1 DSC thermogram of Alloy I in hydrogen,  $15 \text{ K min}^{-1}$ , and enthalpy of hydrogen absorption.

temperature dependence of the exo-maxima on the heating rate, the plot  $\log(\beta/T^2)$  versus  $1/T$  yields a linear plot (Fig. 3a), whose slope gives the activation energy of crystallization,  $E = 349 \pm 7 \text{ kJ mol}^{-1}$ , while the frequency factor, according to Equation 4, is  $Z = 7.7 \times 10^{25} \text{ min}^{-1}$ . Values of crystallization rate constants for some temperatures are shown in Fig. 3b.

##### 3.1.2. Alloy II

The DSC thermograms in a hydrogen flow show that the crystallization (devitrification) process occurs in two steps at rather close temperatures ( $535\text{--}548^\circ\text{C}$ ) as can be seen in Fig. 4. The total enthalpy of crystallization of  $-\Delta H = 70 \text{ J g}^{-1}$  is found after integrating areas of both exo-maxima. Temperature dependences of both exo-maxima yield linear plots as shown in Fig. 5. The corresponding activation energies are  $E_1 = 1193 \pm 247 \text{ kJ mol}^{-1}$  and  $E_2 = 950 \pm 193 \text{ kJ mol}^{-1}$ , and the frequency factors  $Z_1 = 3.6 \times 10^{76} \text{ min}^{-1}$  and  $Z_2 = 3.8 \times 10^{61} \text{ min}^{-1}$ . Temperature changes of the rate constants are shown in Fig. 6. X-ray spectra of amorphous (a) and crystalline (b) samples are presented in Fig. 7.

#### 3.2. Electric and magnetic investigations

The relative change of the electrical resistance was determined, as described in Section 2, from room

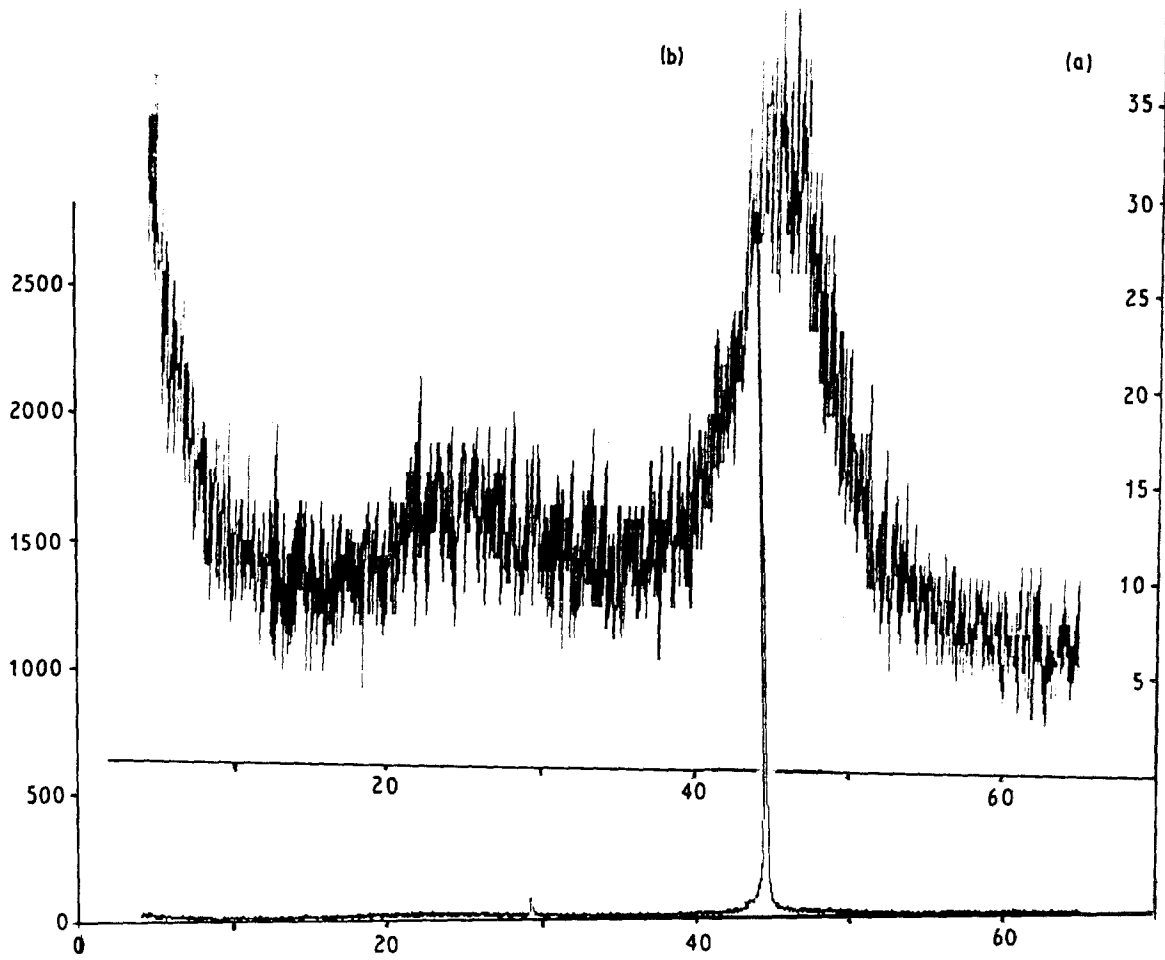


Figure 2 X-ray diffractograms of Alloy I (a) before and (b) after heating (crystallization).

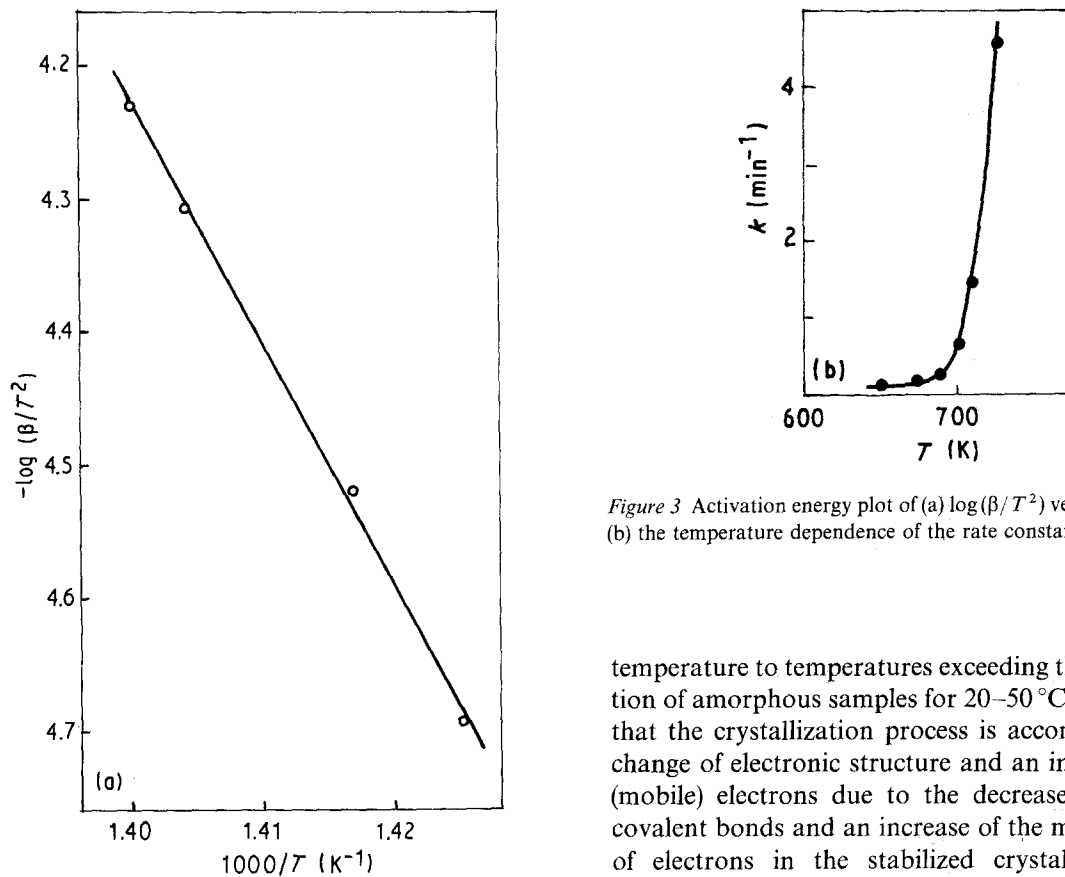


Figure 3 Activation energy plot of (a)  $\log(\beta/T^2)$  versus  $1/T$  (a) and (b) the temperature dependence of the rate constant for Alloy I.

temperature to temperatures exceeding the crystallization of amorphous samples for 20–50 °C. Fig. 8 shows that the crystallization process is accompanied by a change of electronic structure and an increase of free (mobile) electrons due to the decreased number of covalent bonds and an increase of the mean free path of electrons in the stabilized crystal state. It is

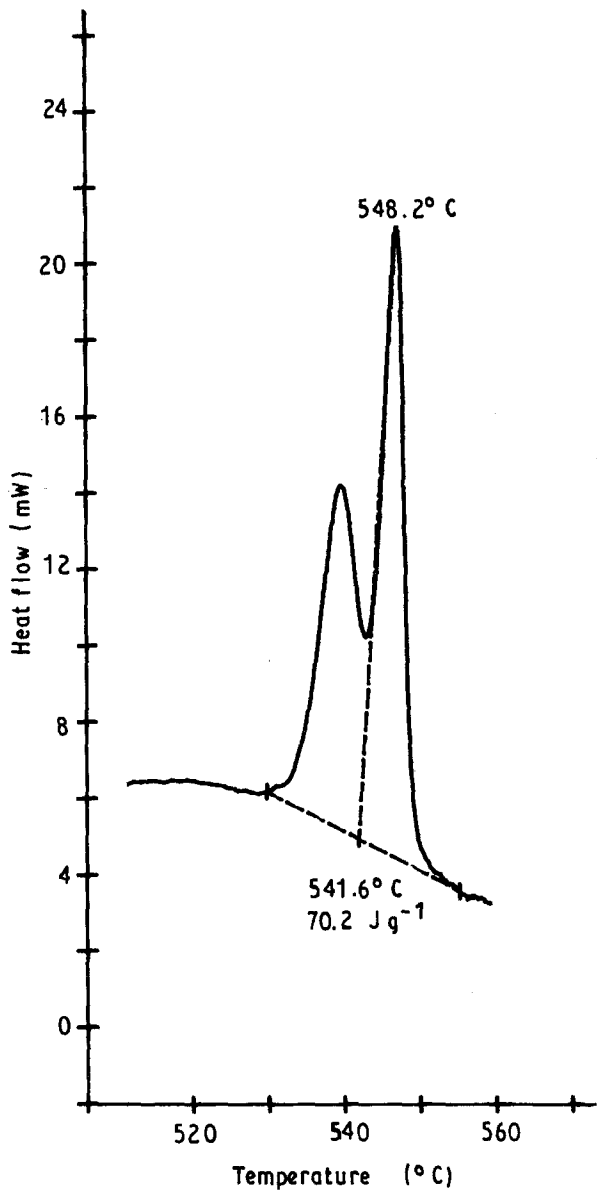


Figure 4 DSC thermogram of Alloy II in hydrogen,  $15 \text{ K min}^{-1}$ , and enthalpy of hydrogen absorption.

noticeable that the biggest change in relative resistance takes place at the temperatures of sample crystallization.

As already mentioned, the changes of the relative magnetic permeabilities of the samples were determined at room temperature. They were first heated to temperatures above the temperature of crystallization. From Fig. 8 it can be seen that the relative magnetic permeability of both magnetics (I and II) follows the change in crystal structure. The main change, a sudden decrease, occurs within the range of crystallization temperatures. Such a behaviour shows that the change of crystal and electronic structures affects the change of the magnetic structure, connected with the distribution of magnetic domains and possibly with different coupling of electron spins, the carriers of magnetic properties.

#### 4. Conclusions

From the results obtained concerning the connections between thermal stability, the crystallization process,

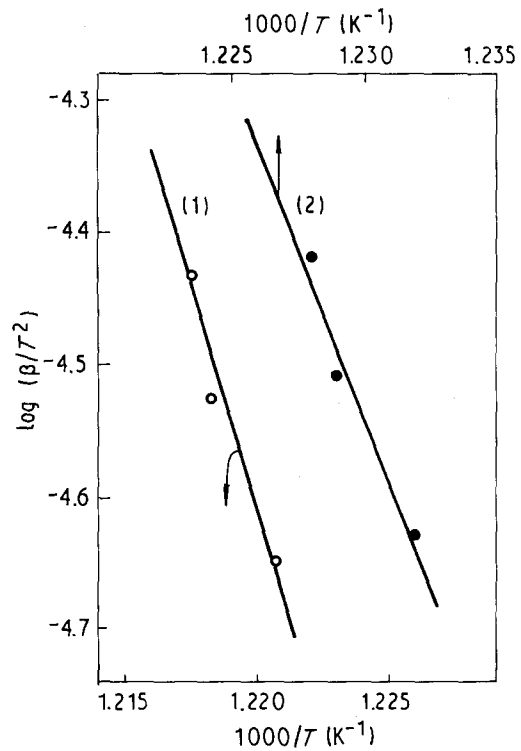


Figure 5 Activation energy plot of  $\log(\beta/T^2)$  versus  $1/T$  for Alloy II: (1) first and (2) second maximum (crystallization step).

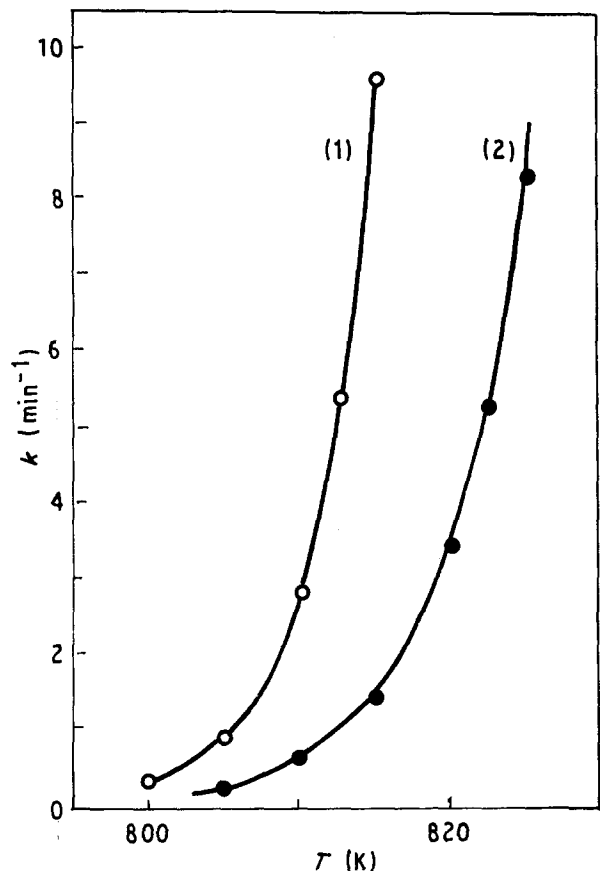


Figure 6 Temperature dependence of the rate constant: (1) first and (2) second crystallization step.

and the changes of electrical resistance and magnetic permeability of amorphous alloys (magnetics), it can be concluded that the thermal stability of the amorphous (glassy) state depends on the composition of the

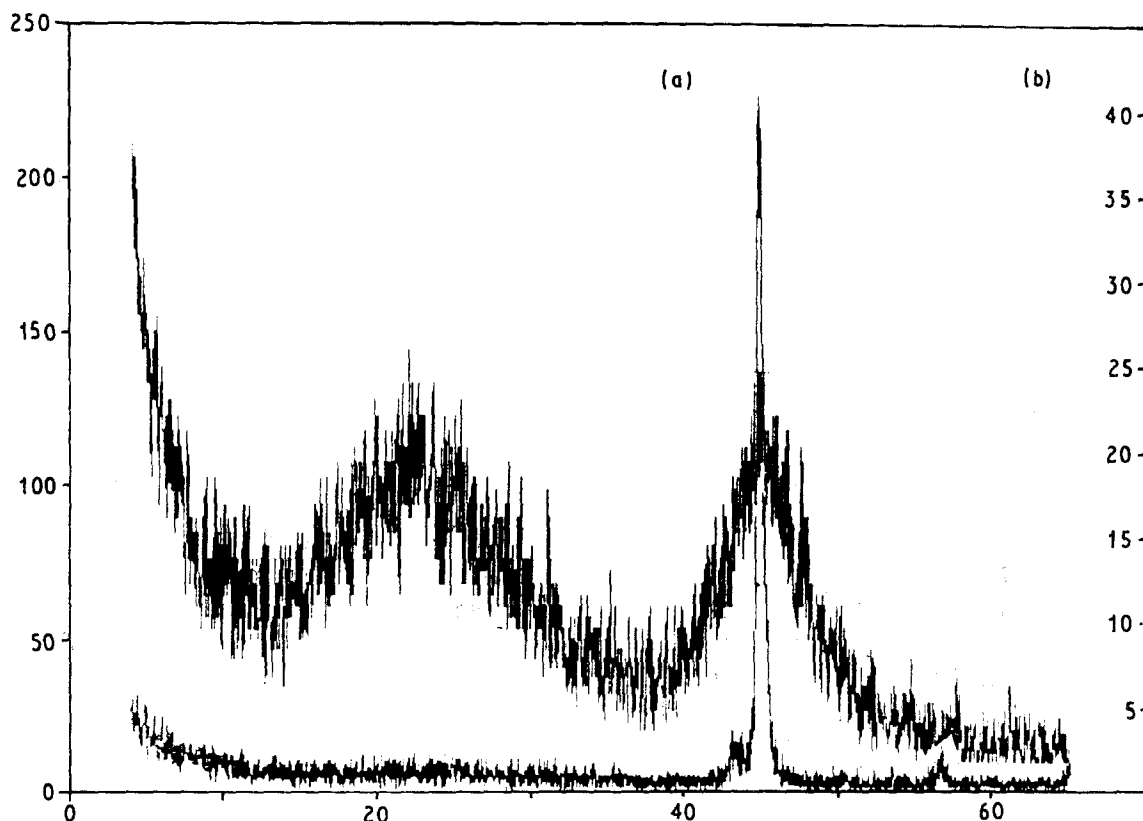


Figure 7 X-ray diffractograms of Alloy II (a) before and (b) after heating (crystallization).

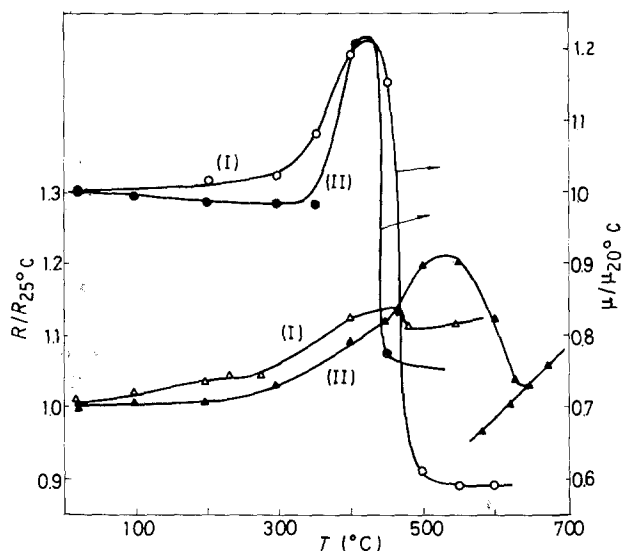


Figure 8 The change of relative electrical resistance and relative magnetic permeability with temperature for Alloys I and II.

investigated Alloys I and II. The crystallization process takes place in one step for Alloy I and in two steps for Alloy II. It can be further concluded that the process of transition of the glassy state into the crystal state is quite complex, causing various changes in electronic and magnetic structures, particularly in the range of crystallization temperatures. The relative electrical resistance and the relative magnetic permeability reach maximum values in the range of crystallization temperatures and then experience abrupt decreases at the end of crystallization. The kinetic analysis shows high values of activation energies and

frequency factors, but rather low values of crystallization rate constants. The enthalpies of crystallization of the exothermal processes range from 50–70 J g<sup>-1</sup>.

## References

1. J. D. BERNAL, *Nature* **185** (1960) 68.
2. S. TAKAYMA, *J. Mater. Sci.* **11** (1976) 164.
3. W. KLEMENT, R. H. WILLENS and P. DUWZ, *Nature* **187** (1969) 869.
4. P. DUWEZ, R. H. WILLENS and W. KLEMENT, *J. Appl. Phys.* **31** (1960) 1136.
5. N. J. GRANT and B. C. GISSEN (eds) in "Rapidly Quenched Metals" (MIT Press, Cambridge, Massachusetts, 1976).
6. D. ADLER, *Sci. Amer.* **236** (1977).
7. U. KÖSTER and U. HEROLD, in "Glassy Metals I", edited by H.-J. Güntherodt and H. Beck (Springer-Verlag Berlin, Heidelberg, New York, 1981) pp. 225–59.
8. F. E. LUBORSKI (ed.), "Amorphous Metallic Alloys" ("amofnye Metallicheskie Splavy") (Butterworths Monographs Materials, London, Boston, Sydney, 1983) (in Russian "Merallurgiya", Moscow, 1987).
9. M. V. ŠUŠIĆ and A. M. MARIČIĆ, *Metalkde*, in press.
10. A. F. ANDREEV, *Zh. Eksper. Teor. Fiz.* **74** (1978) 786.
11. G. S. CARGILL, *Solid State Phys.* **30** (1975) 227.
12. A. T. PEDZIWITER, E. B. BOLTICH, W. E. WALLACE and R. S. CRAIG, in "Electronic Structure and Properties of Hydrogen in Metals", edited by P. Jena and C. B. Satterthwaite, Published in cooperation with NATO Scientific Affairs Division (Plenum Press, New York, London, 1983) pp. 367–72.
13. A. R. FERCHMIN and S. KOBE, "Amorphous Magnetism and Metallic Magnetic Materials Digest" (North-Holland, Amsterdam, New York, Oxford, 1983).
14. M. V. ŠUŠIĆ, *J. Mat. Sci. Lett.* **5** (1986) 1251.

Received 5 October 1990  
and accepted 18 March 1991